Comparative analysis of cortical anatomy in male participants with internet gaming disorder or tobacco use disorder: Insights from normative modeling

XUEFENG MA[1,2†] , ANHANG JIANG[2†] , JUNHONG DAI[2],
SHUANG LI[2], HONGAN CHEN[2], YONG XIE[2],
SHIZHEN WANG[2], BO YANG[2], LINGXIAO WANG[2,3,4] and
GUANG-HENG DONG[1*]

[1] Department of Psychology, Yunnan Normal University, Kunming, Yunnan Province, P.R. China

[2] Center for Cognition and Brain Disorders, School of Clinical Medicine and the Affiliated Hospital of Hangzhou Normal University, Hangzhou, P.R. China

[3] Zhejiang Key Laboratory for Research in Assessment of Cognitive Impairments, Hangzhou, Zhejiang Province, P.R. China

[4] Institutes of Psychological Sciences, Hangzhou Normal University, Hangzhou, Zhejiang Province, P.R. China

ABSTRACT

Background: Research on individual differences in brain structural features of internet gaming disorder (IGD) and established addictions such as tobacco use disorder (TUD) is currently limited. This study utilized normative modeling to analyze the cortical thickness (CT) development patterns of male patients with IGD and TUD, aiming to provide further insights into whether IGD qualifies as an addiction. *Methods:* Surface-based brain morphometry (SBM) was used to calculate CT from T1-weighted magnetic resonance imaging data of 804 male participants (665 healthy individuals, 68 IGD and 71 TUD). Gaussian process regression was employed to generate normative models of CT development. Deviation maps were produced to depict deviations of IGD and TUD participants from the typical developmental patterns. *Results:* Both addiction groups exhibited widespread cortical thinning, particularly in regions such as the bilateral temporal pole and medial orbitofrontal cortex. The TUD group demonstrated a higher degree of individualization and limited spatial overlap compared to the IGD group. Opposite trends in CT changes were observed between the two groups in the bilateral pericalcarine cortex and pars triangularis. *Conclusions:* These findings regarding the similarities and differences between IGD and TUD provide support for the idea that IGD shares common features with substance-related addictions and contribute to a deeper understanding of the neural mechanisms underlying IGD.

†Co-first authors.

*Corresponding author.
E-mail: dongguangheng@ynnu.edu.cn

INTRODUCTION

Internet gaming disorder (IGD) is defined as a psychiatric condition that manifests as a struggle to control excessive and disruptive gaming behaviors (Wang et al., 2023). In 2013, The Diagnostic and Statistical Manual of Mental Disorders, Fifth Edition (DSM-5) classified IGD as a potential psychiatric disorder that needs further study (American Psychiatric

Association, 2013). In 2019, IGD was officially termed as a mental disorder in the 11th revision of the International Classification of Diseases (ICD-11) (ICD-11 for Mortality and Morbidity). Evidence shows that 23% of gamers experience symptoms of internet gaming addiction (Mathews, Morrell, & Molle, 2019), characterized by tolerance, withdrawal, attempts to conceal or lie about gaming activities, negligence toward important life opportunities, and other associated features (Dong, Zheng, Wang, Ye, & Dong, 2022; Wang et al., 2022). Individuals with IGD encounter difficulties in managing their gaming habits, which may have negative consequences such as poor interpersonal relationships, academic failure, emotional distress, and even physical health concerns (Dong & Potenza, 2022; Wan et al., 2022; Ye, Wang, Yang, Dong, & Dong, 2022; Zha et al., 2022). Epidemiological studies conducted in general population have revealed the overall prevalence of IGD to be 0.7–15.6%, with an average proportion of 4.7% over the years (Feng, Ramo, Chan, & Bourgeois, 2017). Research on IGD has consistently highlighted significant gender disparities in its prevalence. Numerous studies have indicated a higher prevalence of IGD among males compared to females (Fam, 2018; Ko, Yen, Chen, Chen, & Yen, 2005; Rehbein, Kliem, Baier, Mößle, & Petry, 2015). In 2022, the DSM-5-TR listed IGD in the section that recommended conditions for further research (not an official one) (American Psychiatric Association, 2022). Therefore, more evidence is needed to support the classification of IGD as an addictive disorder. Investigation of the similarities and differences between IGD and typical addictive disorders, such as Tobacco Use Disorder (TUD), may help researchers better address the ongoing controversies surrounding this issue.

TUD is a prevalent and persistent substance-related disorder characterized by a compulsive and uncontrolled use of tobacco products. Dependency on tobacco products has been associated with over 7 million deaths worldwide annually. Smoking has been shown to shorten life expectancy by about 10 years and directly contribute to approximately two-thirds of all smoking-related deaths. The World Health Organization's eighth report on global tobacco use revealed that, in 2019, the smoking rate was 17.5% among individuals aged 15 years and older. At present, it is estimated that there are 847 million adult male smokers, 153 million adult female smokers, and 24 million smokers aged 13–15 years worldwide. Shen et al.'s longitudinal study on Chinese smokers revealed that the smoking prevalence among males (67.9%) is significantly higher than among females (2.7%) (Shen et al., 2018). Smokers tend to have overall poorer cognitive function in late adulthood than non-smokers, with lower scores in several cognitive domains such as memory and cognitive flexibility (Corley, Gow, Starr, & Deary, 2012). Smoking has, therefore, become a significant public health concern that poses a widespread threat to the global population (Burki, 2021). The choice to compare IGD with TUD is multifaceted. Firstly, both IGD and TUD exhibit similar trends in terms of prevalence and severity within populations, facilitating participant recruitment for studies. Secondly, both disorders demonstrate significant gender disparities, with a higher prevalence among males than females. This gender discrepancy underscores the importance of understanding potential gender-specific risk factors and treatment approaches for these addictive disorders.

Some resting-state functional magnetic resonance imaging (fMRI) studies have attempted to conduct comparative research between the two disorders. A study (Chen et al., 2023) found that IGD and TUD patients exhibit common node strength enhancement between the subcortical and motor networks. In addition, these authors reported common enhanced resting-state functional connectivity (RSFC) between the right thalamus and right postcentral gyrus in both groups of participants. A task-based fMRI study (Ko, 2013) revealed similar mechanisms in cue-induced reactivity for the parahippocampus between IGD and TUD patients. Another RSFC study (Zheng et al., 2022) reported differences in the thalamus and frontostriatal circuits but similar changes in the cerebellum and medial prefrontal cortex regions between the two addiction groups. Despite fMRI studies providing insights into the commonalities and differences in functional connectivity and cue-induced reactivity between IGD and TUD, further exploration of the structural differences between the two remains relatively limited. Alterations in brain structure can reflect the long-term effects of addictive behaviors on brain morphology and organization and serve as biomarkers for addiction vulnerability or treatment response. Therefore, investigating structural differences between IGD and TUD is crucial for advancing our understanding of addictive disorders and providing targeted intervention measures.

Cortical thickness (CT) is a key indicator for measuring the brain structure. Researchers have focused on revealing the relationship between addiction and brain structure, particularly the impact on CT. For instance, Hong et al. (2013) suggested a link between the orbitofrontal cortex (OFC) and pathology of substance and behavioral addictions. These authors reported a significant decrease in the CT of the right lateral OFC, but not that of the left lateral OFC, among IGD subjects. In contrast, studies conducted by Yuan et al. (2013) and Wang et al. (2018) demonstrated a decrease in the CT of the left OFC of IGD subjects as compared to that of healthy controls (HC). These inconsistent findings highlight the need for a better understanding of the changes in the patterns of CT in IGD and reveal the association between alterations in brain structure and IGD (Weinstein, 2017). Studies on CT in TUD patients have suggested that smoking may lead to overall cortical thinning, as primarily observed in lower CT in the frontal, temporal, and parietal cortices, as well as in the insular cortex (Durazzo, Meyerhoff, & Yoder, 2018; Karama et al., 2015; Li et al., 2015). However, a few reports have suggested no differences in insular cortex thickness among smokers (Kühn, Schubert, & Gallinat, 2010). Morales, Ghahremani, Kohno, Hellemann, and London (2014) found a negative correlation between right insular cortex thickness and cigarette craving in young smokers. Voxel-based and surface-based morphometry experiments have enabled precise and detailed investigations of regional and global

alterations in CT associated with TUD. Further investigations are warranted to elucidate the mechanism underlying gray matter alterations and their functional implications.

Research on cerebral structural differences between IGD and TUD patients is scarce, and there is no clear understanding of the underlying neurobiological mechanisms that contribute to these addictions and their potential overlap or distinctiveness in terms of brain structure. Traditional case-control designs applied thus far have predominantly focused on group differences while overlooking individual-level differences. At the individual level, mapping heterogeneous disease phenotypes is crucial to identify accurate and reliable biomarkers of mental disorders.

In this study, we applied a quantitative measurement statistical model called the normative model that maps population or behavioral variables to the brain. It provides estimates of within-cohort variability and compares individuals to normative brain structures within a specific age range. This approach determines the differences between individual patients and the range of health, similar to the use of growth charts in physical medicine. The normative model assumes that diseases can be regarded as extremes of the normal range or deviations from specific aspects of normal functioning. Considering this assumption, the normative model does not dichotomize the cohort like traditional case-reference paradigms but studies the disease at the individual participant level. This technique undoubtedly offers new perspectives for clinical research (Marquand, Rezek, Buitelaar, & Beckmann, 2016; Wolfers et al., 2018). We hypothesized that IGD and TUD patients exhibit similarities in the developmental patterns of CT at the group level while bearing heterogeneity in certain brain regions and individual levels. We validated this hypothesis by applying the normative model to quantitatively estimate regional brain structural changes in IGD and TUD patients. We examined the spatial overlap with deviations from the normative models to quantitatively estimate the regional brain structural changes in IGD and TUD patients, and to depict similarities and differences in CT development patterns at the level of these disorders and individual patients.

To this end, this study aims to expand our knowledge regarding the neural mechanism of IGD and TUD by investigating CT development patterns. The findings will enhance our understanding of the neurobiological basis of substance-related disorders and non-substance-related disorders and contribute to identify potential brain-based biomarkers to refine diagnostic criteria. This approach will also allow more accurate identification and classification of addiction disorders.

METHODS AND MATERIALS

Participants

78 male individuals with IGD and 80 male individuals with TUD were enrolled in this study, participants with both IGD and TUD were excluded by verbal inquiries before recruitment. The diagnosis of IGD was based on the diagnostic criteria outlined in DSM-5 (Petry et al., 2014) and scores obtained from the Young's Internet Addiction Test (IAT). The IGD status is defined as meeting at least 5 DSM-5 criteria and having an IAT score greater than 50. The standard criteria for TUD diagnosis are same as those used in our previous study (Zheng et al., 2022): (1) Smoke at least 10 cigarettes per day continuously for one year or more; (2) Exhaled carbon monoxide levels were at least 5 ppm; (3) The scores on Fagerström Test for Nicotine Dependence (FTND) are higher than 4 (Ghahremani, Faulkner, Cox, & London, 2018; Loughead et al., 2015); (4) The scores on the 10-item brief Questionnaire on Smoking Urges (QSU-B) are higher than 15 (Sweitzer et al., 2014). The above criteria are considered collectively. Prior to recruiting participants with a particular addiction, we used verbal inquiries to exclude other types of addictions (such as internet gaming, tobacco, alcohol, drugs, etc.). In addition, data of 665 male participants were downloaded from the Brain Genomics Superstruct Project (GSP), a large-scale, multi-site brain imaging study (Holmes et al., 2015). Each site participating in the GSP had obtained informed consent from the participants (view at https://dataverse.harvard.edu/dataset.xhtml?persistentId=doi:10.7910/DVN/25833) prior to their enrolment. Age and education level matching was performed on the groups using the non-parametric nearest neighbor matching procedure provided by the MatchIt package in R (https://cran.r-project.org/web/packages/MatchIt/index.html), resulting in the exclusion of 2 participants from the TUD group. The quality control process conducted based on weighted average image quality rating (IQR) and Euler index yielded a final sample of 68 participants in the IGD group, 71 participants in the TUD group, and 665 participants in the HC group (Fig. 1A). The demographic information of participants is presented in Table 1.

MRI acquisition

High-resolution T1 structural images were acquired on a 3 Tesla Siemens Trio scanner using a fast spoiled gradient-recalled echo pulse sequence with magnetization preparation, which encompassed the entire brain (176 slices). The acquisition parameters were as follows: repetition time (TR), 2,000 ms; echo time (TE), 3 ms; slice thickness, 1.0 mm without any gap; skip, 0 mm; flip angle, 7°; inversion time, 1,100 ms; field of view (FOV), 256×256 mm; in-plane resolution, 256×256.

CT estimation

Raw MRI images were processed and analyzed using surface-based brain morphometry (SBM) pipeline available in the CAT-12 toolbox (Gaser, Nenadic, Buchsbaum, Hazlett, & Buchsbaum, 2001). The images were then integrated in the statistical parametric mapping version 12 (SPM-12) (Fig. 1B) and subjected to pre-processing steps. The volumes were subsequently segmented using surface-based and thickness estimation techniques to analyze specific regions
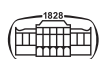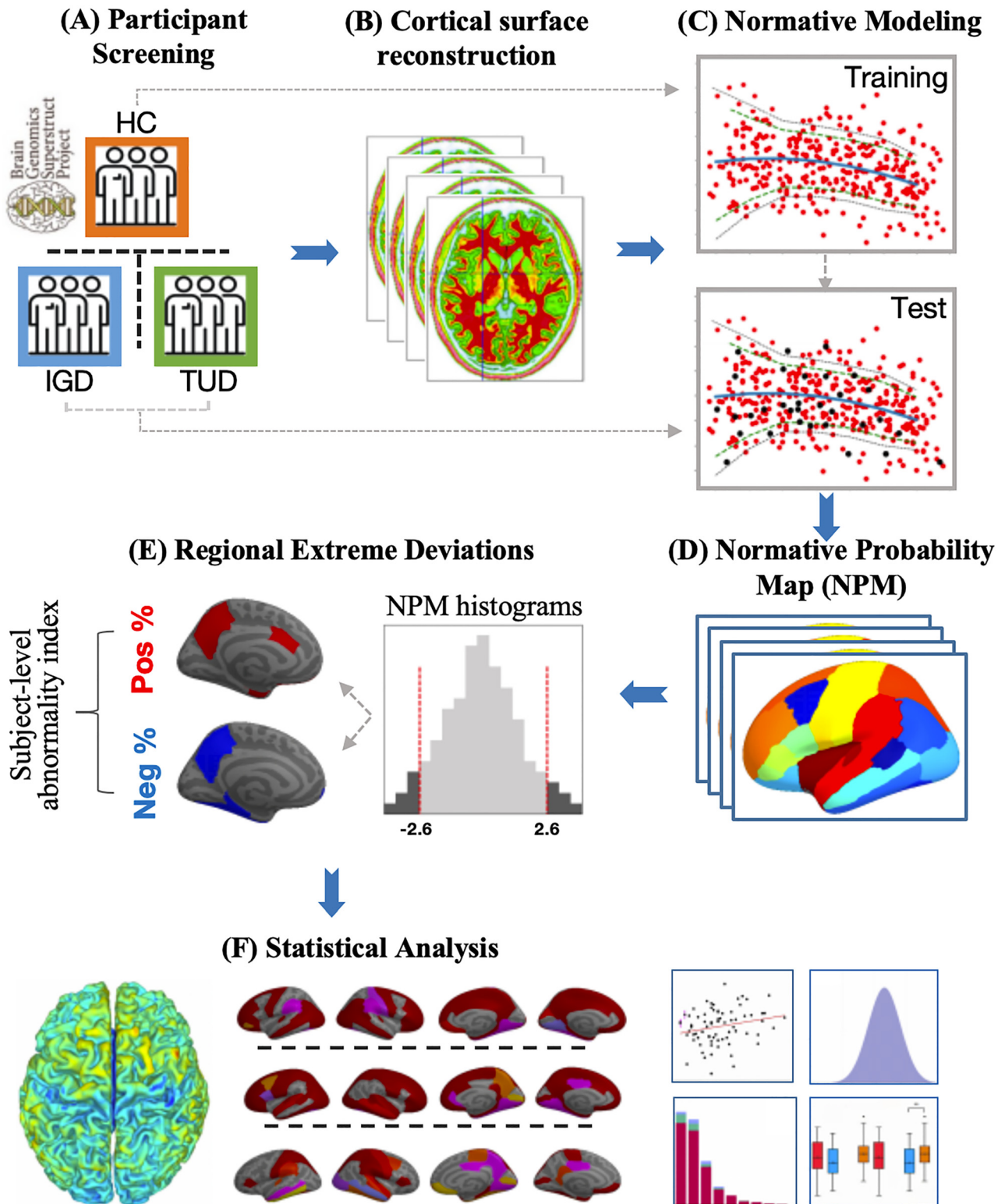
Fig. 1. Methodological overview. A) T1 data were collected from both IGD and TUD patients and age-matched with HC data from the GSP dataset. B) CT data, based on the Desikan-Killiany atlas, were obtained for each participant through cortical surface reconstruction. C) Gaussian process regression was applied, and CT normative models were computed using 10-fold cross-validation. The models were applied to each group of participants. D) NPMs were created for quantifying the deviation (Z-scores) of each participant from the normative models. E) A threshold of z = ±2.6 was used to define extreme values, and its proportion served as an subject-level abnormality index. F) Statistical analyses of various metrics

Table 1. Demographic information of subjects in the current study

	HC $n = 665$	IGD $n = 68$	TUD $n = 71$	F	p
Age (year), M±SD [range]	21.65 ± 3.04 [19–35]	21.46 ± 2.22 [19–29]	22.13 ± 1.80 [19–26]	1.09	0.337
Education (year), M±SD [range]	14.47 ± 1.93 [12–20]	14.38 ± 1.56 [12–18]	13.92 ± 1.73 [9–20]	2.76	0.063
Euler, M±SD [range]	28.41 ± 10.55 [6–64]	29.43 ± 11.71 [14–80]	30.87 ± 11.76 [12–77]	2.11	0.102
DSM, M±SD	NA	6.21 ± 1.13	NA	NA	NA
IAT, M±SD	NA	66.33 ± 9.42	NA	NA	NA
FTND, M±SD	NA	NA	6.58 ± 1.60	NA	NA
QSU, M±SD	NA	NA	27.73 ± 10.61	NA	NA

Abbreviations: NA, not applicable; M, mean; SD, standard deviation; HC, Healthy Control; IGD, Internet Gaming Disorder; TUD, Tobacco Use Disorder; DSM, number of DSM-5 item; IAT, Internet Addiction Test; QSU, Questionnaire for Smoking Urges.

of interest. Cortical parcellation was conducted using the Desikan-Killiany atlas (Desikan et al., 2006). The quality control process was performed by referring to the weighted average IQR assessed by the CAT-12 toolbox, which provides a comprehensive evaluation of the cortical surface reconstruction quality. All participants with IQR ratings below 'C-' were excluded (no participants were excluded in HC, while 8 were excluded in the IGD and 1 in the TUD). CAT-12 also calculates the Euler index, which tallies the instances when the toolbox has interpolated surface gaps during the process of reconstruction to ensure a continuous outcome surface. The index serves as a measure of the reliability of the surface reconstruction and the resulting CT estimates. As the Euler index is closely related to the scanning site, we followed the approach proposed by Rutherford et al. to apply a consistent exclusion threshold across different sites. In this approach, we subtracted the median Euler index of each site from every participant within it, then took the square root and multiplied by −1, and excluded participants with square roots greater than 10. Finally, we manually examined participants that exceeded the Euler index threshold to confirm their exclusion from further processing (no participants were excluded in HC, while 2 were excluded in the IGD and 6 in the TUD).

Normative modeling

The Predictive Clinical Neuroscience toolkit (PCNtoolkit) (https://github.com/predictive-clinical-neuroscience/PCNtoolkit-demo.git) was used to estimate a normative model of CT and predict the entire brain based on participants' age and euler index as covariates. The model estimated using Gaussian process regression (GPR) generated, in addition to point estimates, coherent measures of prediction confidence (Marquand et al., 2016). The normative range of the model in the HC group was estimated through 10-fold cross-validation and then applied to patients (Fig. 1C). A normative probability map (NPM) was then created and applied to each subject by quantifying the deviation of mean CT at each region of interest (ROI) from the normative model and estimating a subject-specific Z score. This allowed us to estimate patterns of regional deviation from typical CT for each participant (Fig. 1D). The z-score takes into account the predicted uncertainty, and reflects the difference between predicted and actual values. To directly compare the deviations of the

cohorts, parameters were estimated using training data with empirical Bayesian estimation (Marquand et al., 2016). Cross-validation ensured the unbiased estimation across different cohorts. Therefore, the mean group differences were determined by performing ROI-level *t*-tests on the z-scores of the three cohorts. Bonferroni-Holm correction was applied for multiple comparisons ($p < 0.05$).

Mapping regional extreme deviations

The z-scores within the ROIs were averaged for each cohort, and the brain regions with larger mean deviations from the normative model were visualized. Different patterns of changes in CT in different regions of the brain were determined from comparison of mean deviations, which revealed specific characteristics of each addiction group. The spatial overlap of individuals in extreme deviations was demonstrated by defining extreme positive and negative deviations from the norm at a threshold of z = ±2.6 (i.e., $p < 0.005$). A fixed statistical significance threshold was chosen to simplify comparisons across individuals and to be less sensitive to overall changes in individual deviation from the norm as compared to methods such as false discovery rate (FDR) correction (Wolfers et al., 2018). The spatial overlap of extreme deviations across groups was investigated by calculating the overlap maps from the proportion of extreme positive and negative deviations within each ROI. This resulted in brain regions where each group exhibited significant increases or decreases relative to normative CT. This method provides a more intuitive representation of the distribution of extreme regional deviations in the brain (Fig. 1E).

Construction of subject-level abnormality index

Normative models can provide probabilistic interpretations of deviations in all participants. Therefore, normative probabilistic maps (NPMs) provide multivariate measurements of all brain regions that deviate from the normative range (Zabihi et al., 2019). The percentage of extreme deviations in each ROI was calculated for each participant and presented as a summary score, including the percentage of extreme positive deviations and percentage of extreme negative deviations (Fig. 1E). We defined extreme average deviations from the model at the threshold of z = ±1.65 (i.e., $p < 0.05$) to identify spatial distribution differences in
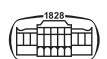
CT deviations from the normative model across groups. Additionally, we visualized regions with extreme deviations exceeding 2% threshold across groups to visualize the key regions of interest (Fig. 1F).

Diagnostic associations

Calculate the Spearman correlation coefficient ($p < 0.05$, FDR corrected) between regional deviations (Z-scores) and severity scores of addiction symptoms (DSM and FTND) through partial correlation analysis (excluding the effects of gender, head motion, and Euler index). All analyses were performed using Python software, version 3.8 (Python Software Foundation). The effects of scanner artifacts were mitigated by performing additional checks (Fig. 1F).

Ethics

This study protocol was approved by the Ethics Investigation Committee of Hangzhou Normal University. All participants provided written informed consent as per the principles outlined in the Declaration of Helsinki.

RESULTS

Comparison of group-level deviations

Figure 2 shows the average group differences in CT relative to the standard model among the HC group (under cross-validation) and the addiction groups after application of Bonferroni correction. Both IGD and TUD groups exhibited broad negative deviations as compared with the HC group. However, the IGD group showed significant average positive deviations in regions such as bilateral frontal pole (IGD-HC, $t = 10.31$, $p_{bonferroni} < 0.001$, left; IGD-HC, $t = 10.35$, $p_{bonferroni} < 0.001$, right) and right superior parietal cortex (IGD-HC, $t = 3.34$, $p_{bonferroni} < 0.001$) (Fig. 2A). Further, the TUD group showed significant positive deviations in regions such as bilateral frontal pole (TUD-HC, $t = 4.11$, $p_{bonferroni} < 0.001$, left; TUD-HC, $t = 6.11$, $p_{bonferroni} < 0.001$, right) and bilateral lateral occipital cortex (TUD-HC, $t = 3.65$, $p_{bonferroni} = 0.001$, left; TUD-HC, $t = 6.40$, $p_{bonferroni} < 0.001$, right) as compared with the HC group (Fig. 2B).

The comparison of between-group deviations in the IGD and TUD groups shows that both groups of patients exhibit similar overall CT deviations. However, the IGD group exhibits greater positive deviations compared to the TUD group in more brain regions, such as bilateral pars triangularis (IGD-TUD, $t = 4.05$, $p_{bonferroni} < 0.001$, left; IGD-TUD, $t = 4.50$, $p_{bonferroni} < 0.001$, right) and the left frontal pole (IGD-TUD, $t = 3.36$, $p_{bonferroni} < 0.001$). In bilateral pericalcarine cortex (IGD-TUD, $t = -5.44$, $p_{bonferroni} < 0.001$, left; IGD-TUD, $t = -3.45$, $p_{bonferroni} < 0.001$, right) and bilateral lingual gyrus (IGD-TUD, $t = -4.59$, $p_{bonferroni} < 0.001$, left; IGD-TUD, $t = -2.09$, $p_{bonferroni} = 0.042$, right), the TUD group
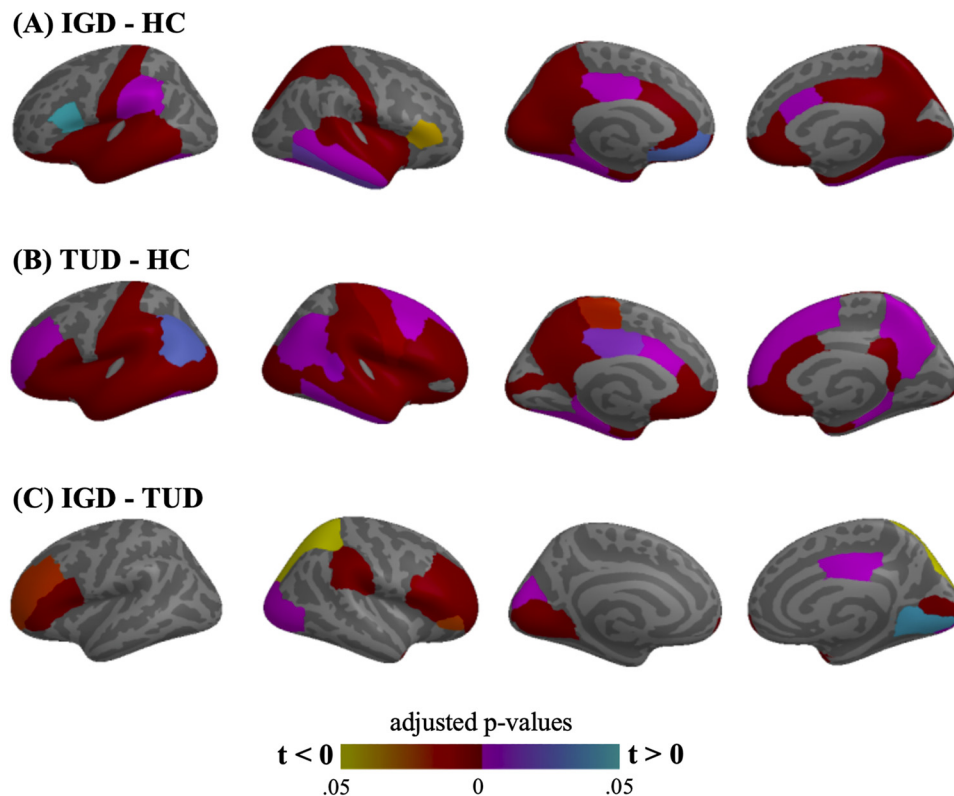

Fig. 2. Intergroup differences in deviations from the normative model. Pairwise comparisons of normative deviations between each group in A-C to visualize regions with significant differences ($p_{Bonferroni} < 0.05$). The color bars represent adjusted *p*-values

demonstrates significantly more negative deviations compared to the IGD group (Fig. 2C).

Noteworthy, different developmental trends were recorded between the two addiction groups in the bilateral pericalcarine cortex and bilateral pars triangularis. In the pericalcarine cortex, the IGD group showed significant negative deviation (IGD-HC, $t = -7.82$, $p_{bonferroni} < 0.001$, left; IGD-HC, $t = -6.48$, $p_{bonferroni} < 0.001$, right) and the TUD group exhibited a significant positive deviation (TUD-HC, $t = 3.35$, $p_{bonferroni} = 0.003$, left; TUD-HC, $t = 0.965$, $p_{bonferroni} = 1$, right) as compared to the HC group. In the pars triangularis, the IGD group showed significant positive deviation (IGD-HC, $t = 1.16$, $p_{bonferroni} = 0.759$, left; IGD-HC, $t = 2.50$, $p_{bonferroni} = 0.041$, right) and the TUD group exhibited a significant negative deviation (TUD-HC, $t = -4.97$, $p_{bonferroni} < 0.001$, left; TUD-HC, $t = -4.40$, $p_{bonferroni} < 0.001$, right) as compared to the HC group. All results are reported in Supplementary Table S1.

Spatial extent of extreme deviations

At a threshold Z value of 1.65 ($p = 0.05$), the HC group in general did not show significant deviations from the normative model, indicating the good fit of this model for this queue. The analysis of extreme positive deviations reveals that the TUD group has a notably higher proportion, accounting for 20.59% (14/68) of the ROIs examined, compared to the IGD group, which only accounts for 8.82% (6/68). Similarly, in terms of extreme negative deviations, the TUD group exhibits a substantially higher proportion, comprising 73.53% (50/68) of the ROIs, compared to the IGD group, which constitutes 42.65% (29/68) of the ROIs.

Figure 3A displays the negative mean deviations from the normative model in the IGD group in the left temporal pole ($Z = -1.82$). As seen in the overlap plot of the IGD group, the proportions of positive deviations were higher in the regions such as bilateral frontal pole (left 10.29%; right 17.65%), bilateral precentral gyrus (left 2.94%; right 5.88%) and superior parietal cortex (right 2.94%). In addition, there were higher proportions of negative deviations in the regions such as lateral temporal pole (left −23.53%; right −19.12%), lateral insula (left −11.76%; right −10.29%) and bilateral pericalcarine cortex (left −10.29%; right −11.76%).

Figure 3B depicts the negative mean deviations from the normative model observed in the TUD group (consistent with that in the IGD group) in the left temporal pole ($Z = -2.00$). The TUD group also exhibited larger average negative deviations in the right temporal pole ($Z = -2.22$) and right medial orbitofrontal cortex ($Z = -1.76$). Meanwhile, the IGD group also showed a trend of decreased average CT in the right temporal pole ($Z = -1.59$) and right medial orbitofrontal cortex ($Z = -1.38$). The overlap plot of the TUD group demonstrated higher proportions of positive deviations in the regions such as bilateral frontal pole (left 7.04%; right 4.23%), bilateral precentral gyrus (left 4.23%; right 9.86%), bilateral superior parietal cortex (left 4.23%; right 2.82%) and bilateral pericalcarine cortex (left 11.27%; right 8.45%). On the other hand, he TUD

group showed a higher proportion of negative deviations in almost whole brain, especially in the lateral temporal pole (left −30.99%; right −39.44%), bilateral superior temporal (left −25.35%; right −15.49%), bilateral medial orbitofrontal cortex (left −2.82%; right −19.72%) and insula (left −14.08%), which closely matches the brain regions with the highest proportion of deviations observed in the IGD group. All results are reported in Supplementary Table S2 and Table S3.

Association with symptoms

In the IGD group, a positive correlation was observed between DSM scores and the regional Z-scores of the left entorhinal cortex ($r = 0.27$, $p_{FDR} = 0.029$), right lateral orbitofrontal cortex ($r = 0.25$, $p_{FDR} = 0.041$), right parahippocampal gyrus ($r = 0.25$, $p_{FDR} = 0.004$) and right frontal pole ($r = 0.26$, $p_{FDR} = 0.036$) (see Fig. 4A). The TUD group, on the other hand, FTND scores were negatively correlated with the regional Z-scores of the left lateral orbitofrontal cortex ($r = -0.24$, $p_{FDR} = 0.047$), right medial orbitofrontal cortex ($r = -0.38$, $p_{FDR} = 0.001$), right rostral anterior cingulate cortex ($r = -0.28$, $p_{FDR} = 0.016$), right rostral middle frontal gyrus ($r = -0.25$, $p_{FDR} = 0.039$), left superior parietal cortex ($r = -0.29$, $p_{FDR} = 0.015$) and left superior temporal cortex ($r = -0.27$, $p_{FDR} = 0.023$) (see Fig. 4B).

DISCUSSION

Herein, we applied normative modeling to compare the deviations in CT development patterns between IGD and TUD individuals relative to a typical control group. Our results show that the TUD group exhibited overall brain atrophy and that the IGD group showed a similar overall trend but slightly lower degree of defects. On one hand, the two groups of patients exhibit a high degree of alignment in the distribution of CT extreme values; on the other hand, the average deviations and regional specificity differences observed between the two addiction groups demonstrate a highly individualized pattern that deviated from the traditional case-control paradigm and manifested differently at different developmental stages.

Similar deviation trends and the concentration of extreme values

Consistent with previous findings, we observed widespread cortical thinning in patients with IGD and TUD compared to the HC group. Our study further revealed that both the IGD and TUD groups exhibited significant average negative deviations and a high proportion of extreme deviations in the bilateral temporal pole and medial orbitofrontal cortex. The temporal pole is known to play a crucial role in social cognition, emotion processing, and decision-making (Olson, McCoy, Klobusicky, & Ross, 2013; Olson, Plotzker, & Ezzyat, 2007). Dysfunction in this region has been linked to impulsivity and altered reward processing, which are
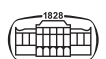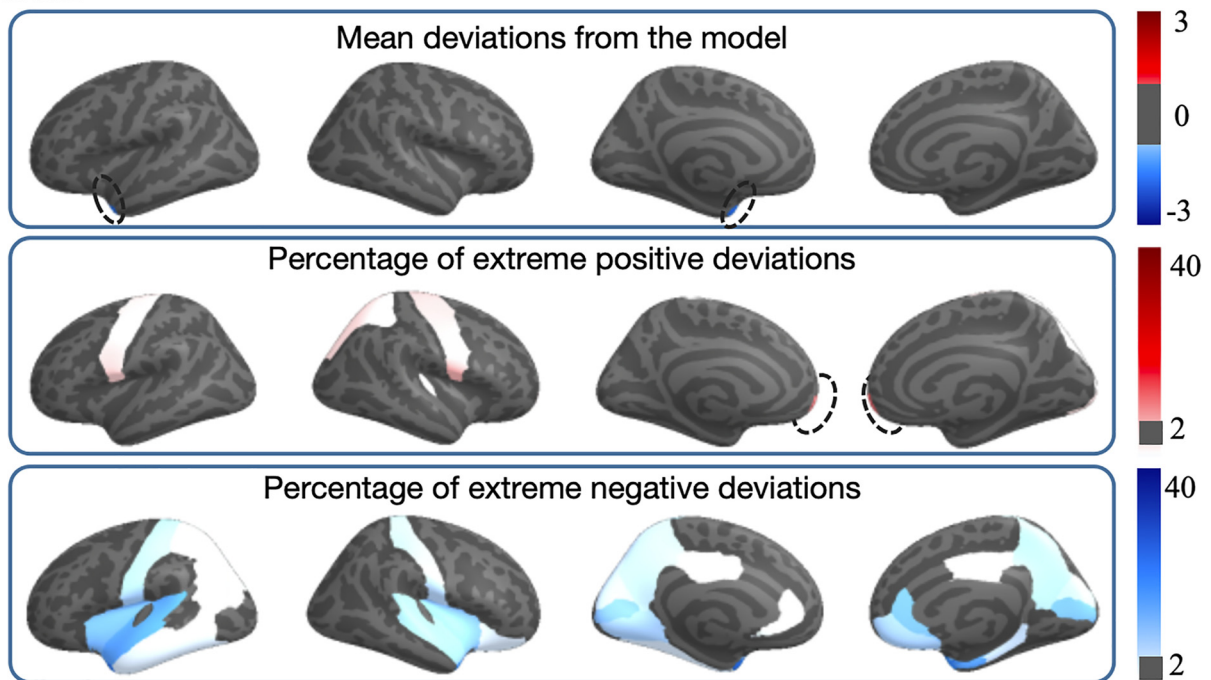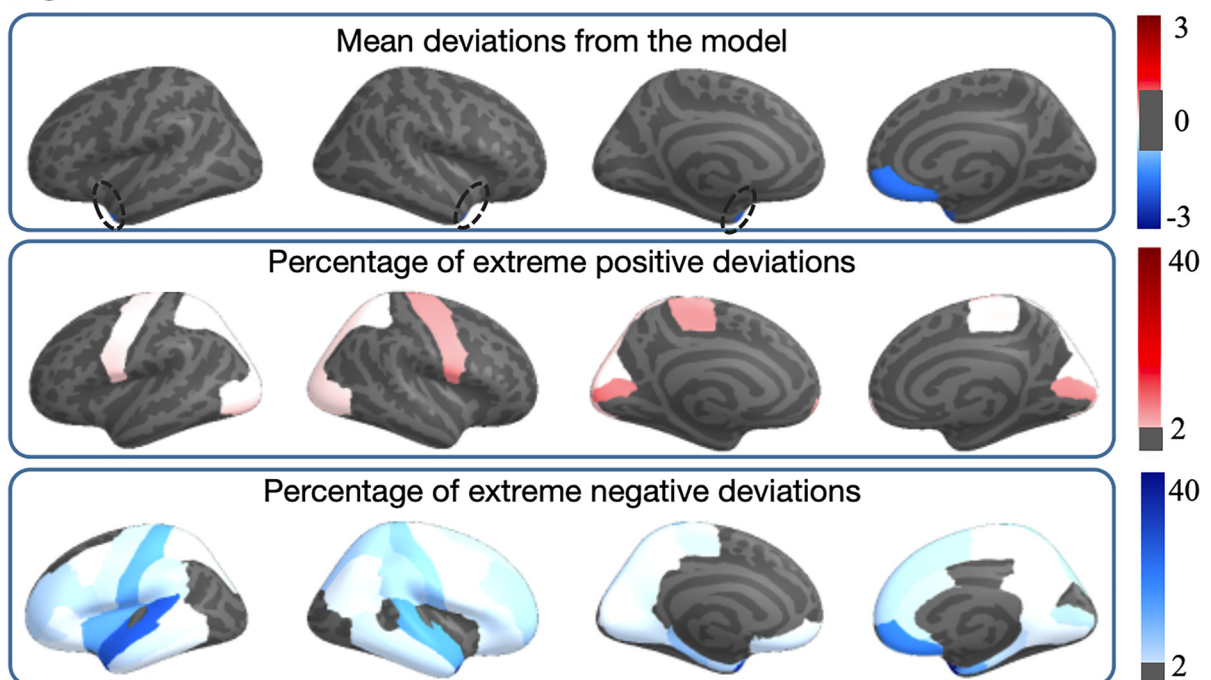
(A) IGD

(B) TUD

Fig. 3. Spatial overlap of extreme deviations. A-B, Map of the regional extreme deviations in two addiction groups. The upper panel displays the region with higher mean deviations from the normative model, and the two lower panels show the region with higher proportion of extreme positive and negative deviations from the normative model

relevant features of addictive behaviors (Camchong, Mac-Donald, Bell, Mueller, & Lim, 2011). Similarly, the medial orbitofrontal cortex is implicated in reward processing, value-based decision-making, and behavioral control (Rolls, 2019; Wallis, 2007). Disruptions in these brain regions may contribute to the development and maintenance of addictive behaviors seen in IGD and TUD. Our findings underscore

the potential utility of these regions as neuroimaging bio-markers for addiction. Future studies should investigate the functional implications of these structural alterations and their relationship to clinical characteristics and treatment outcomes in IGD and TUD populations.

The spatial distribution of extreme CT deviations in both addiction groups exhibits certain overlap, with extreme
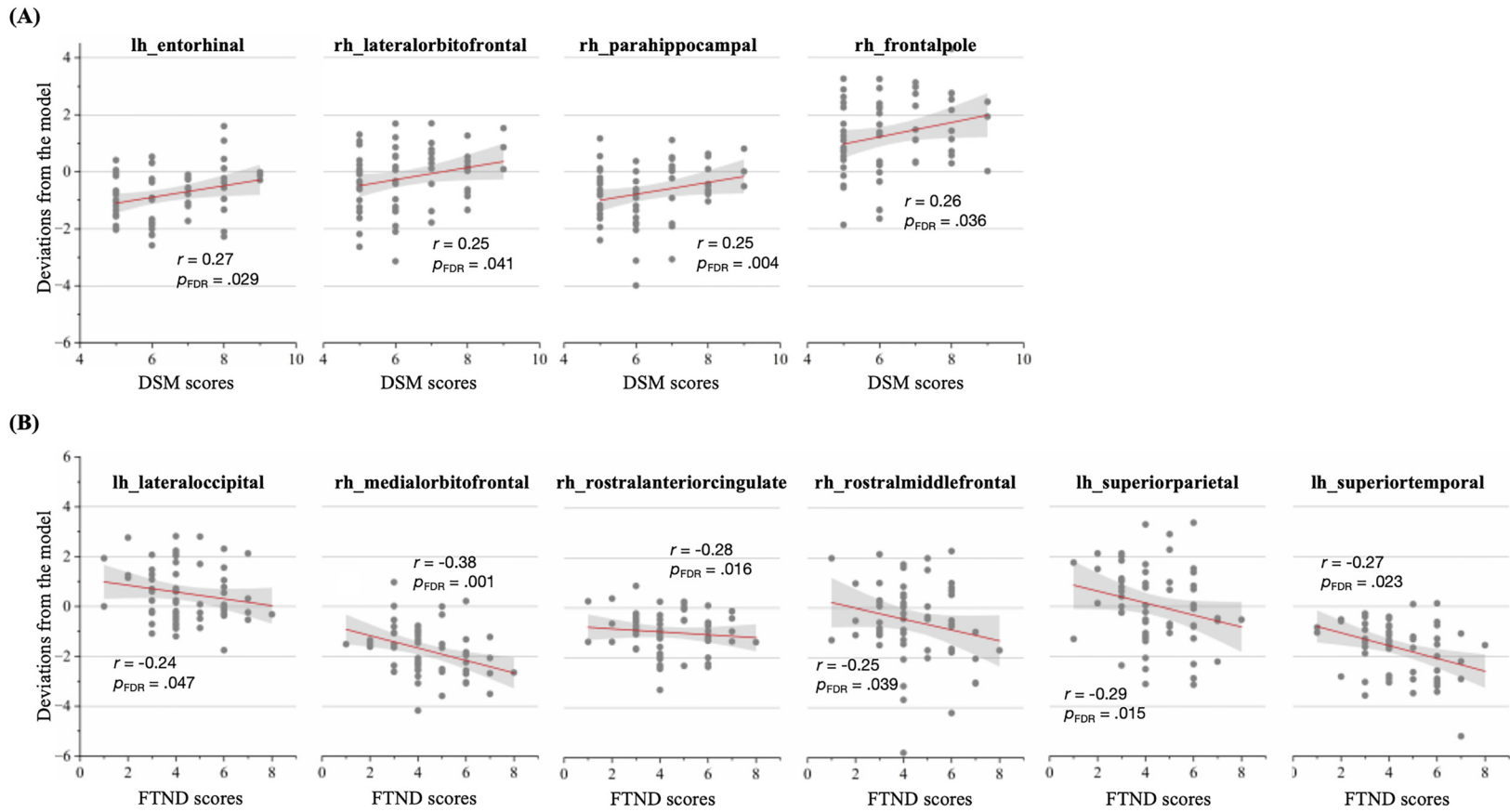
Fig. 4. Partial correlation analysis. A) Correlations between regional deviations and DSM scores. B) Correlations between regional deviations and FTND scores

positive deviations predominantly concentrated in bilateral frontal pole regions, while extreme negative deviations are concentrated in areas such as the insula, temporal pole, and superior temporal gyrus. Correlation analyses revealed a positive association between the right frontal pole CT deviation in the IGD group and their DSM scores. Similarly, the left superior temporal gyrus CT deviation in the TUD group showed a positive correlation with their FTND scores. The elevated CT in the frontal pole among both groups may suggest compensatory mechanisms or neuroadaptive responses to addictive behaviors, potentially reflecting alterations in executive functions and decision-making processes (George & Koob, 2017; Goldstein & Volkow, 2011). These changes may have potential significance in assessing and monitoring the severity of addiction and treatment outcomes (Schacht, Anton, & Myrick, 2013). Furthermore, the spatial convergence of extreme negative deviations in regions implicated in reward processing and emotion regulation, such as the insula and temporal pole, underscores their critical role in addiction pathology (Naqvi & Bechara, 2010). These findings suggest shared neurobiological alterations in specific brain regions implicated in addiction-related behaviors among individuals with IGD and TUD, underscoring the clinical relevance of these neuroimaging markers in assessing addiction severity and treatment outcomes.

Specificity and heterogeneity in the CT development patterns

Although both addiction groups exhibited widespread cortical thinning, the TUD group generally deviated from the model to a greater extent than the IGD group. Nicotine exposure is known to impact cortical structure and function, affecting regions involved in cognitive control and decision-making (Koob & Volkow, 2016). In contrast, the patterns observed in IGD may be related to excessive and compulsive gaming behaviors, which can also impact brain structure and function, albeit possibly through different mechanisms (Kuss, Griffiths, Karila, & Billieux, 2014; Weinstein & Lejoyeux, 2010). This observation may be attributed to the fact that substances can have a greater impact on brain structure alteration than behavioral addictions. The direct introduction of psychoactive substances into the body leads to neurochemical imbalances and subsequent structural changes in key brain regions involved in reward, decision-making, and emotional regulation. On the other hand, behavioral addictions primarily affect functional connectivity patterns, and their influence on structural alterations may be less pronounced (Corley et al., 2012; Li et al., 2015; Morales et al., 2014).

Compared to the IGD group, the TUD group exhibits a higher degree of heterogeneity in whole-brain CT deviations. Specifically, the TUD group shows a simultaneous presence of more extreme positive and negative deviations in regions such as the paracentral lobule, pericalcarine cortex, precentral gyrus, and frontal pole, while the IGD group demonstrates a more uniform deviations across whole brain

regions. Additionally, the TUD group displays a broader range of CT abnormalities, with TUD group having higher proportions of extreme ROIs compared to the IGD group. The increased variability in CT deviations in the TUD group may reflect the diverse neurobiological mechanisms of tobacco addiction and its impact on brain structure. The relationship between the degree of heterogeneity and diagnosis awaits further investigation.

The observed differences in CT development trajectories between individuals with IGD and those with TUD, particularly in the bilateral pericalcarine cortex and bilateral pars triangularis, highlight intriguing neurobiological distinctions associated with these diseases. In our study, we found that the IGD group exhibited significantly positive deviations in the bilateral pericalcarine cortex compared to the HC group, whereas the TUD group showed significantly negative deviations in this region relative to HC group. This finding suggests potential neuroadaptive processes specific to IGD, potentially related to visual processing and sensory integration, which have been previously associated with alterations in the pericalcarine cortex (Maguire, 2001; Murray, Wise, & Drevets, 2011). In the bilateral pars triangularis, the two groups exhibited the opposite pattern compared to the above, with IGD group exhibiting significantly negative deviations and TUD group showing significantly positive deviations relative to HC group. The pars triangularis is known to be involved in cognitive control and language processing (Amunts et al., 1999), and our findings may reflect distinct patterns of neural plasticity associated with different addictive behaviors. These differential CT patterns in the pericalcarine cortex and pars triangularis may be related to underlying neural mechanisms specific to IGD and TUD. For instance, the observed increased CT in the pericalcarine cortex among individuals with IGD could be associated with heightened attentional and perceptual processes, potentially related to gaming-related visual stimuli (Kuss & Griffiths, 2012). Conversely, the reduced CT in the pars triangularis in IGD may reflect alterations in cognitive control and decision-making processes commonly impaired in addiction (Goldstein & Volkow, 2011). Further research is needed to elucidate the precise mechanisms underlying these cortical thickness alterations and their implications for understanding and treating addictive behaviors.

In conclusion, this study employed a normative modeling approach to investigate similarities and differences in the cortical anatomy of IGD and TUD individuals. This approach preserved the traditional case-control paradigm for group-level analyses while simultaneously provided an additional insight at a more individualized level. Thus, it contributed to personalized addiction research. Our findings demonstrate widespread commonalities among two disorders where extreme individual differences are otherwise masked by averaged group-level deviations. These outlier individuals are meaningful in themselves, and using normative modeling to identify and explain these individual-level differences is not only a statistical advancement but also a valuable approach to gather important information on neurobiological substrates of addiction-related processes.

This enables us to move beyond reliance on diagnoses and gain a better understanding of the heterogeneity of mental disorders.

Limitations

Our study has some limitations. Firstly, the analysis was performed on an ROI-wise rather than vertex-wise basis. This approach facilitates comparison of structural abnormalities between regions but may result in the loss of more local information. Secondly, this study only excluded participants with other types of addiction through verbal inquiry before recruitment, lacking scale and biochemical data for intergroup comparisons. Thirdly, the GSP dataset does not provide diagnoses for IGD and TUD, so some participants in the dataset may have IGD or TUD. Despite the enormous sample size of GSP, it may still potentially affect the results of normative modeling. Lastly, the trajectory of brain development was based on the cross-sectional data, and further research is warranted to validate these findings in longitudinal cohorts.

CONCLUSIONS

Herein we developed a model of cortical development using a large HC cohort and applied it to IGD and TUD cohorts to quantify the extent of patients' deviations. Our results indicate that the CT development patterns in IGD and TUD patients exhibited consistent large-scale deviations (primarily cortical atrophy). IGD and TUD patients demonstrated heterogeneity at the individual level, characterized by high individualization and limited spatial overlap. The PCC was the only brain region where different CT developmental trends were observed between the two groups. These findings will improve our knowledge of the neural mechanisms underlying IGD and broaden our ideas about the pathophysiology of substance-related versus non-substance-related disorders.

Authors' contribution: XM and AJ analyzed the study data, prepared the figures and tables, and wrote the initial draft (including substantive translation). JD, SL, HC, YX, SW contributed to the research idea and data analyses. BY contributed to data collection and organization. LW and GHD participated in editing, interpretation, and revision. All authors contributed to and have approved the final manuscript.

SUPPLEMENTARY MATERIALS

Supplementary data to this article can be found online at https://doi.org/10.1556/2006.2024.00044.

REFERENCES

American Psychiatric Association (2013). *Diagnostic and statistical Manual of mental disorders* (5th ed.).

American Psychiatric Association (2022). *Diagnostic and statistical Manual of mental disorders* (5th ed.). *Text Revision*. Washington, DC: American Psychiatric Association.

Amunts, K., Schleicher, A., Bürgel, U., Mohlberg, H., Uylings, H. B., & Zilles, K. (1999). Broca's region revisited: Cytoarchitecture and intersubject variability. *The Journal of Comparative Neurology, 412*(2), 319–341. https://doi.org/10.1002/(sici)1096-9861(19990920)412:2<319::aid-cne10>3.0.co;2-7.

Burki, T. K. (2021). WHO releases latest report on the global tobacco epidemic. *The Lancet Oncology, 22*(9), 1217. https://doi.org/10.1016/S1470-2045(21)00464-2.

Camchong, J., MacDonald, A. W., Bell, C., Mueller, B. A., & Lim, K. O. (2011). Altered functional and anatomical connectivity in schizophrenia. *Schizophrenia Bulletin, 37*(3), 640–650. https://doi.org/10.1093/schbul/sbp131.

Chen, H., Zha, R., Lai, X., Liu, Y., Wei, Z., Wang, M., … Zhang, X. (2023). Internet gaming disorder and tobacco use disorder share neural connectivity patterns between the subcortical and the motor network. *Human Brain Mapping, 44*(6), 2607–2619. https://doi.org/10.1002/hbm.26233.

Corley, J., Gow, A. J., Starr, J. M., & Deary, I. J. (2012). Smoking, childhood IQ, and cognitive function in old age. *Journal of Psychosomatic Research, 73*(2), 132–138. https://doi.org/10.1016/j.jpsychores.2012.03.006.

Desikan, R. S., Ségonne, F., Fischl, B., Quinn, B. T., Dickerson, B. C., Blacker, D., … Killiany, R. J. (2006). An automated labeling system for subdividing the human cerebral cortex on MRI scans into gyral based regions of interest. *NeuroImage, 31*(3), 968–980. https://doi.org/10.1016/j.neuroimage.2006.01.021.

Dong, G. H., & Potenza, M. N. (2022). Considering gender differences in the study and treatment of internet gaming disorder. *Journal of Psychiatric Research, 153*, 25–29. https://doi.org/10.1016/j.jpsychires.2022.06.057.

Dong, H., Zheng, H., Wang, M., Ye, S., & Dong, G. H. (2022). The unbalanced behavioral activation and inhibition system
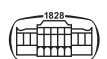
sensitivity in internet gaming disorder: Evidence from resting-state Granger causal connectivity analysis. *Progress in Neuropsychopharmacology & Biological Psychiatry*, 119, 110582. https://doi.org/10.1016/j.pnpbp.2022.110582.

Durazzo, T. C., Meyerhoff, D. J., & Yoder, K. K. (2018). Cigarette smoking is associated with cortical thinning in anterior frontal regions, insula and regions showing atrophy in early Alzheimer's Disease. *Drug and Alcohol Dependence*, 192, 277–284. https://doi.org/10.1016/j.drugalcdep.2018.08.009.

Fam, J. Y. (2018). Prevalence of internet gaming disorder in adolescents: A meta-analysis across three decades. *Scandinavian Journal of Psychology*, 59(5), 524–531. https://doi.org/10.1111/sjop.12459.

Feng, W., Ramo, D. E., Chan, S. R., & Bourgeois, J. A. (2017). Internet gaming disorder: Trends in prevalence 1998-2016. *Addictive Behaviors*, 75, 17–24. https://doi.org/10.1016/j.addbeh.2017.06.010.

Gaser, C., Nenadic, I., Buchsbaum, B. R., Hazlett, E. A., & Buchsbaum, M. S. (2001). Deformation-based morphometry and its relation to conventional volumetry of brain lateral ventricles in MRI. *Neuroimage*, 13(6 Pt 1), 1140–1145. https://doi.org/10.1006/nimg.2001.0771.

George, O., & Koob, G. F. (2017). Individual differences in the neuropsychopathology of addiction. *Dialogues in Clinical Neuroscience*, 19(3), 217–229. https://doi.org/10.31887/DCNS.2017.19.3/gkoob.

Ghahremani, D. G., Faulkner, P. M., Cox, C., & London, E. D. (2018). Behavioral and neural markers of cigarette-craving regulation in young-adult smokers during abstinence and after smoking. *Neuropsychopharmacology*, 43(7), 1616–1622. https://doi.org/10.1038/s41386-018-0019-7.

Goldstein, R. Z., & Volkow, N. D. (2011). Dysfunction of the prefrontal cortex in addiction: Neuroimaging findings and clinical implications. *Nature Reviews Neuroscience*, 12(11). https://doi.org/10.1038/nrn3119.

Holmes, A. J., Hollinshead, M. O., O'Keefe, T. M., Petrov, V. I., Fariello, G. R., Wald, L. L., … Buckner, R. L. (2015). Brain Genomics Superstruct Project initial data release with structural, functional, and behavioral measures. *Scientific Data*, 2, 150031. https://doi.org/10.1038/sdata.2015.31.

Hong, S. B., Kim, J. W., Choi, E. J., Kim, H. H., Suh, J. E., Kim, C. D., … Yi, S. H. (2013). Reduced orbitofrontal cortical thickness in male adolescents with internet addiction. *Behavioral and Brain Functions: BBF*, 9, 11. https://doi.org/10.1186/1744-9081-9-11.

ICD-11 for mortality and morbidity statistics. Accessed June 24, 2023. https://icd.who.int/browse11/l-m/en#/http%3A%2F%2Fid.who.int%2Ficd%2Fentity%2F1448597234.

Karama, S., Ducharme, S., Corley, J., Chouinard-Decorte, F., Starr, J. M., Wardlaw, J. M., … Deary, I. J. (2015). Cigarette smoking and thinning of the brain's cortex. *Molecular Psychiatry*, 20(6), 778–785. https://doi.org/10.1038/mp.2014.187.

Ko, C. H. (2013). The brain activations for both cue-induced gaming urge and smoking craving among subjects comorbid with Internet gaming addiction and nicotine dependence. *Journal of Psychiatric Research*, 47(4), 486–493. https://doi.org/10.1016/j.jpsychires.2012.11.008.

Ko, C. H., Yen, J. Y., Chen, C. C., Chen, S. H., & Yen, C. F. (2005). Gender differences and related factors affecting online gaming addiction among Taiwanese adolescents. *The Journal of Nervous and Mental Disease*, 193(4). https://doi.org/10.1097/01.nmd.0000158373.85150.57.

Koob, G. F., & Volkow, N. D. (2016). Neurobiology of addiction: A neurocircuitry analysis. *Lancet Psychiatry*, 3(8), 760–773. https://doi.org/10.1016/S2215-0366(16)00104-8.

Kühn, S., Schubert, F., & Gallinat, J. (2010). Reduced thickness of medial orbitofrontal cortex in smokers. *Biological Psychiatry*, 68(11), 1061–1065. https://doi.org/10.1016/j.biopsych.2010.08.004.

Kuss, D. J., & Griffiths, M. D. (2012). Internet gaming addiction: A systematic review of empirical research. *International Journal of Mental Health and Addiction*, 10(2), 278–296. https://doi.org/10.1007/s11469-011-9318-5.

Kuss, D. J., Griffiths, M. D., Karila, L., & Billieux, J. (2014). Internet addiction: A systematic review of epidemiological research for the last decade. *Current Pharmaceutical Design*, 20(25), 4026–4052. https://doi.org/10.2174/13816128113199990617.

Li, Y., Yuan, K., Cai, C., Feng, D., Yin, J., Bi, Y., … Tian, J. (2015). Reduced frontal cortical thickness and increased caudate volume within fronto-striatal circuits in young adult smokers. *Drug and Alcohol Dependence*, 151, 211–219. https://doi.org/10.1016/j.drugalcdep.2015.03.023.

Loughead, J., Wileyto, E. P., Ruparel, K., Falcone, M., Hopson, R., Gur, R., & Lerman, C. (2015). Working memory-related neural activity predicts future smoking relapse. *Neuropsychopharmacology*, 40(6), 1311–1320. https://doi.org/10.1038/npp.2014.318.

Maguire, E. A. (2001). The retrosplenial contribution to human navigation: A review of lesion and neuroimaging findings. *Scandinavian Journal of Psychology*, 42(3), 225–238. https://doi.org/10.1111/1467-9450.00233.

Marquand, A. F., Rezek, I., Buitelaar, J., & Beckmann, C. F. (2016). Understanding heterogeneity in clinical cohorts using normative models: Beyond case-control studies. *Biological Psychiatry*, 80(7), 552–561. https://doi.org/10.1016/j.biopsych.2015.12.023.

Mathews, C. L., Morrell, H. E. R., & Molle, J. E. (2019). Video game addiction, ADHD symptomatology, and video game reinforcement. *The American Journal of Drug and Alcohol Abuse*, 45(1), 67–76. https://doi.org/10.1080/00952990.2018.1472269.

Morales, A. M., Ghahremani, D., Kohno, M., Hellemann, G. S., & London, E. D. (2014). Cigarette exposure, dependence, and craving are related to insula thickness in young adult smokers. *Neuropsychopharmacology*, 39(8), 1816–1822. https://doi.org/10.1038/npp.2014.48.

Murray, E. A., Wise, S. P., & Drevets, W. C. (2011). Localization of dysfunction in major depressive disorder: Prefrontal cortex and amygdala. *Biological Psychiatry*, 69(12). https://doi.org/10.1016/j.biopsych.2010.09.041.

Naqvi, N. H., & Bechara, A. (2010). The insula and drug addiction: An interoceptive view of pleasure, urges, and decision-making. *Brain Structure & Function*, 214(5–6), 435–450. https://doi.org/10.1007/s00429-010-0268-7.

Olson, I. R., McCoy, D., Klobusicky, E., & Ross, L. A. (2013). Social cognition and the anterior temporal lobes: A review and theoretical framework. *Social Cognitive and Affective Neuroscience*, 8(2). https://doi.org/10.1093/scan/nss119.

Olson, I. R., Plotzker, A., & Ezzyat, Y. (2007). The enigmatic temporal pole: A review of findings on social and emotional processing. *Brain*, 130(Pt 7), 1718–1731. https://doi.org/10.1093/brain/awm052.

Petry, N. M., Rehbein, F., Gentile, D. A., Lemmens, J. S., Rumpf, H.-J., Mößle, T., … O'Brien, C. P. (2014). An international consensus for assessing internet gaming disorder using the new DSM-5 approach. *Addiction*, 109(9), 1399–1406. https://doi.org/10.1111/add.12457.

Rehbein, F., Kliem, S., Baier, D., Mößle, T., & Petry, N. M. (2015). Prevalence of internet gaming disorder in German adolescents: Diagnostic contribution of the nine DSM-5 criteria in a statewide representative sample. *Addiction*, 110(5), 842–851. https://doi.org/10.1111/add.12849.

Rolls, E. T. (2019). The cingulate cortex and limbic systems for emotion, action, and memory. *Brain Structure & Function*, 224(9), 3001–3018. https://doi.org/10.1007/s00429-019-01945-2.

Rutherford, S., Kia, S. M., Wolfers, T., Fraza, C., Zabihi, M., Dinga, R., … Marquand, A. F. (2022). The normative modeling framework for computational psychiatry. *Nature Protocols*, 17(7), 1711–1734. https://doi.org/10.1038/s41596-022-00696-5.

Schacht, J. P., Anton, R. F., & Myrick, H. (2013). Functional neuroimaging studies of alcohol cue reactivity: A quantitative meta-analysis and systematic review. *Addiction Biology*, 18(1), 121–133. https://doi.org/10.1111/j.1369-1600.2012.00464.x.

Shen, Q., Zhu, N. B., Yu, C. Q., Guo, Y., Bian,, Z., Tan, Y. L., … China Kadoorie Biobank (CKB) Collaborative Group (2018). Sex-specific associations between tobacco smoking and risk of cardiovascular diseases in Chinese adults. *Zhonghua Liu Xing Bing Xue Za Zhi*, 39(1), 8–15. https://doi.org/10.3760/cma.j.issn.0254-6450.2018.01.002.

Sweitzer, M. M., Geier, C. F., Joel, D. L., McGurrin, P., Denlinger, R. L., Forbes, E. E., & Donny, E. C. (2014). Dissociated effects of anticipating smoking versus monetary reward in the caudate as a function of smoking abstinence. *Biological Psychiatry*, 76(9), 681–688. https://doi.org/10.1016/j.biopsych.2013.11.013.

Wallis, J. D. (2007). Orbitofrontal cortex and its contribution to decision-making. *Annual Review of Neuroscience*, 30, 31–56. https://doi.org/10.1146/annurev.neuro.30.051606.094334.

Wan, L., Zha, R., Ren, J., Li, Y., Zhao, Q., Zuo, H., & Zhang, X. (2022). Brain morphology, harm avoidance, and the severity of excessive internet use. *Human Brain Mapping*, 43(10), 3176–3183. https://doi.org/10.1002/hbm.25842.

Wang, Z. L., Song, K. R., Zhou, N., Potenza, M. N., Zhang, J. T., & Dong, G. H. (2022). Gender-related differences in involvement of addiction brain networks in internet gaming disorder: Relationships with craving and emotional regulation. *Progress in Neuro-psychopharmacology & Biological Psychiatry*, 118, 110574. https://doi.org/10.1016/j.pnpbp.2022.110574.

Wang, Z., Wu, L., Yuan, K., Hu, Y., Zheng, H., Du, X., & Dong, G. (2018). Cortical thickness and volume abnormalities in Internet gaming disorder: Evidence from comparison of recreational Internet game users. *The European Journal of Neuroscience*, 48(1), 1654–1666. https://doi.org/10.1111/ejn.13987.

Wang, L., Zhang, Z., Wang, S., Wang, M., Dong, H., Chen, S., … Dong, G. (2023). Deficient dynamics of prefrontal-striatal and striatal-default mode network (DMN) neural circuits in internet gaming disorder. *Journal of Affective Disorders*, 323, 336–344. https://doi.org/10.1016/j.jad.2022.11.074.

Weinstein, A. M. (2017). An update overview on brain imaging studies of internet gaming disorder. *Front Psychiatry*, 8, 185. https://doi.org/10.3389/fpsyt.2017.00185.

Weinstein, A., & Lejoyeux, M. (2010). Internet addiction or excessive internet use. *The American Journal of Drug and Alcohol Abuse*, 36(5), 277–283. https://doi.org/10.3109/00952990.2010.491880.

Wolfers, T., Doan, N. T., Kaufmann, T., Alnæs, D., Moberget, T., Agartz, I., … Marquand, A. F. (2018). Mapping the heterogeneous phenotype of schizophrenia and bipolar disorder using normative models. *JAMA Psychiatry*, 75(11), 1146. https://doi.org/10.1001/jamapsychiatry.2018.2467.

Ye, S., Wang, M., Yang, Q., Dong, H., & Dong, G. H. (2022). Predicting the severity of internet gaming disorder with resting-state brain features: A multi-voxel pattern analysis. *Journal of Affective Disorders*, 318, 113–122. https://doi.org/10.1016/j.jad.2022.08.078.

Yuan, K., Cheng, P., Dong, T., Bi, Y., Xing, L., Yu, D., … Tian, J. (2013). Cortical thickness abnormalities in late adolescence with online gaming addiction. *Plos One*, 8(1), e53055. https://doi.org/10.1371/journal.pone.0053055.

Zabihi, M., Oldehinkel, M., Wolfers, T., Frouin, V., Goyard, D., Loth, E., … Marquand, A. F. (2019). Dissecting the heterogeneous cortical anatomy of autism spectrum disorder using normative models. *Biological Psychiatry: Cognitive Neuroscience and Neuroimaging*, 4(6), 567–578. https://doi.org/10.1016/j.bpsc.2018.11.013.

Zha, R., Li, P., Liu, Y., Alarefi, A., Zhang, X., & Li, J. (2022). The orbitofrontal cortex represents advantageous choice in the Iowa gambling task. *Human Brain Mapping*, 43(12), 3840–3856. https://doi.org/10.1002/hbm.25887.

Zheng, Y., Dong, H., Wang, M., Zhou, W., Lin, X., & Dong, G. (2022). Similarities and differences between internet gaming disorder and tobacco use disorder: A large-scale network study. *Addiction Biology*, 27(2). https://doi.org/10.1111/adb.13119.